

# Flexible Electronics Toward Wearable Sensing

Wei Gao,<sup>1,\*</sup> Hiroki Ota,<sup>2,\*</sup> Daisuke Kiriya,<sup>3,\*</sup> Kuniharu Takei,<sup>3,\*</sup> Ali Javey<sup>4,5,6\*</sup>

<sup>1</sup> Division of Engineering and Applied Science, California Institute of Technology, Pasadena, CA, United States

<sup>2</sup> Department of Systems integration, Yokohama National University, Yokohama, Japan

<sup>3</sup> Department of Physics and Electronics, Osaka Prefecture University, Osaka, Japan

<sup>4</sup> Department of Electrical Engineering and Computer Sciences, University of California, Berkeley, CA, USA

<sup>5</sup> Berkeley Sensor and Actuator Center, University of California, Berkeley, CA, USA

<sup>6</sup> Materials Sciences Division, Lawrence Berkeley National Laboratory, Berkeley, CA, USA

\* ajavey@berkeley.edu, weigao@caltech.edu, ota-hiroki-xm@ynu.ac.jp, kiriya@pe.osakafu-u.ac.jp, takei@pe.osakafu-u.ac.jp.

**Conspectus:** Wearable sensors play a crucial role in realizing personalized medicine as they can continuously collect data from the human body and to capture meaningful health status changes in time for preventive intervention. However, motion artifacts and mechanical mismatches between conventional rigid electronic materials and soft skin often lead to substantial sensor errors during epidermal measurement. Owing to its

unique properties such as high flexibility and conformability, flexible electronics enables a natural interaction between electronics and the human body. In this Account, we will summarize our recent studies on the design of flexible electronic devices and systems for physical and chemical monitoring. Material innovation, sensor design, device fabrication, system integration, and human studies employed toward continuous and non-invasive wearable sensing will be discussed.

Flexible electronic device typically contains several key components including the substrate, the active layer, and the interface layer. The inorganic nanomaterials-based active layer (prepared by physical transfer or solution process) is shown to have high physicochemical properties, electron/hole mobility, and mechanical strength. Flexible electronics based on the printed and transferred active materials has shown great promise for physical sensing. For example, integrating a nanowire transistor array for the active matrix and a conductive pressure-sensitive rubber enables tactile pressure mapping; tactile pressure-sensitive e-skin and organic light emitting diodes can be integrated for instantaneous pressure visualization. Such printed sensors have been applied as wearable patches to monitor skin temperature, ECG and human activities. In addition, liquid metals could serve as an attractive candidate for flexible electronics owing to their excellent conductivity, flexibility, and stretchability. Liquid metal enabled electronics (based on liquid-liquid heterojunctions and embedded

microchannels) have been utilized for monitoring a wide range of physiological parameters (e.g., pulse and temperature).

Despite the rapid growth in wearable sensing technologies, there is an urgent need of developing flexible devices that can capture molecular data from the human body to retrieve more insightful health information. We have developed a wearable and flexible sweat sensing platform toward real-time multiplexed perspiration analysis. An integrated iontophoresis module on wearable sweat sensor could enable autonomous and programmed sweat extraction. A microfluidic-based sensing system was demonstrated for sweat sampling, sensing, and sweat rate analysis. Roll-to-roll gravure printing allows for mass production of high-performance flexible chemical sensors at low cost. These wearable & flexible sweat sensors have shown great promise in dehydration monitoring, cystic fibrosis diagnosis, drug monitoring, and non-invasive glucose monitoring.

Future work in this field should focus on designing robust wearable sensing systems to accurately collect data from the human body, and on large-scale human studies to determine how the measured physical and chemical information relate to the individual's specific health conditions. Further research in these directions, along with the large sets of data collected *via* these wearable and flexible sensing technologies, will have a significant impact on future personalized healthcare.

## **1. Introduction**

Wearable electronics are expected to play a crucial role in personalized medicine as they continuously and closely monitor an individual's physical activities and health status. Owing to its high flexibility and conformability, flexible electronics could serve as an ideal platform for designing future personalized wearable devices.<sup>1-4</sup> Emerging nanotechnology and materials science have recently led to remarkable development in flexible electronics for personalized healthcare. In this Account, we will focus on the very recent advances of flexible electronics from our group for both physical and chemical sensing. In the following sections, we will review material innovation, device fabrication, sensor design and system integration employed toward non-invasive wearable sensing systems. Finally, the overall challenges and opportunities that lie ahead for flexible electronic skin on the road towards personalized health monitoring will be discussed.

## **2 Materials and device fabrication**

**Figure 1** illustrates a typical configuration of the flexible electronic device: the key components are the substrate, the active layer, and the interface layer between them. The substrate is the base to build up devices, the active layer is materials or electrical circuits to add functionalities, and the interface is important in some cases to keep the active layers on or inside the substrates (e.g., adhesion of SWCNTs on substrates shown below). These layers should be well designed for designated targets.

Active layers, composed of materials or electrical components on the e-skin to add functionalities, are critical to constructing devices on the flexible substrate. Organic materials have been widely explored as a flexible device material.<sup>5</sup> In contrast, inorganic nanomaterials have high physicochemical properties, high electron/hole mobility, chemical durability, and mechanical strength; they can also be applied as an active material to construct flexible devices through standard lithography processes. For example, carbon nanotubes (CNTs)<sup>6</sup> and graphene<sup>7</sup> have been utilized as an active layer of field-effect transistors (FETs) and sensors, and semiconducting crystalline nanowires show high-performance FETs on flexible substrates.<sup>8-10</sup> Composite materials (e.g., CNTs and Ag nanoparticle composites) can also be applied as an active conductive layer on flexible and stretchable substrates.<sup>11</sup> To achieve effective construction of the active layers, the interface layer between the active layer and the substrate is also critical, especially for FET operation (**Figure 1**). In the case of single-walled carbon nanotube (SWCNT) metal-oxide-semiconductor FETs (MOSFETs), the interface is critical to achieve gate controllability.<sup>12,13</sup> A thin single-layer network of SWCNTs is required to control the electrostatic operation of MOSFET, which is obtained only when SWCNTs and the substrates are in an attractive condition on the designed interface layer.<sup>14</sup> Owing to their excellent conductivity, flexibility, and stretchability, liquid metals are expected to enable conformal coverage on curved and soft surfaces of electronic systems that will have applications in wearable sensors, robotics, and prosthetics.<sup>15</sup> Gallium metal alloys,

particularly eutectic gallium indium (EGaIn) and Galinstan (Ga/In/Sn), are among the most widely used liquid metals in electrical components including electrodes and sensors (**Figure 1**).<sup>16</sup> They are ideal materials for designing a stretchable and flexible electronic skin. Under extreme stretching, twisting and bending, unlike contacts based on solid metals and polymers which will experience cracking or disconnection, the liquid metal electrodes and interconnections can act as a “self-healing” wire and maintain good electrical performance because of their fluidity.<sup>17-20</sup>

The choice for the transfer process of the active layers onto the substrates is dependent on the preparation process of the materials to the active layers. As illustrated in **Figures 2 and 3**, the physical transfer and solution processes have been explored. In the physical transfer method, nanowires directly contact with substrates and are transferred in an aligned manner (**Figure 2**). For example, Ge nanowires grown vertically on flat donor substrates can be transferred via mechanical shearing to an acceptor substrate (**Figure 2a**),<sup>9</sup> or Ge nanowires grown on a metal roller can be transferred to the substrate *via* mechanical roll-contact (**Figure 2b**).<sup>9,21</sup> These nanowire arrays can be patterned with further photolithography and lift-off processes. The nanowire array was realized on a 4-inch wafer, glass, paper and a flexible polyethylenimine (PEI) substrate (**Figure 2c-e**), and showed high optoelectronic performance.<sup>8,22</sup> Due to electrostatic and van der Waals interaction forces, the nanowires can be transferred onto any

surfaces, including flexible substrates. These uniform nanowire active layers can serve as high mobility transistor channels to construct e-skins.

Solution transfer processes have been widely applied to construct active layers for flexible electronics due to their lower temperature and greater suitability for mass-productive printing technology.<sup>23-25</sup> To form a printable ink by mixing nanomaterials and organic materials, wettability and adhesion of inks on the targeted surface should be considered.<sup>11,14</sup> SWCNT solutions were developed as a printable ink. It is inevitable to consider that SWCNTs are wrapped with surfactants to prohibit aggregation in the solution (ink); therefore, to effectively form the active layer, the design of the interaction between the surfactant and the substrate is critical (**Figures 3a and 3b**).<sup>12,14</sup> In order to assemble FET-grade SWCNT network, the areal density of the randomly deposited SWCNTs should be higher than the percolation limit between electrodes.<sup>26</sup> Furthermore, it should be a sufficiently thin single-layer; otherwise, it is difficult to modulate carriers to operate FETs due to the metallic behaviors of bundled SWCNTs. An effective deposition method was developed using cholate surfactants, such as sodium cholate (SC) to prepare SWCNT inks combined with the designed substrate modified with amine-terminated interlayers, such as poly-L-lysine (PLL) and (3-Aminopropyl)triethoxysilane (APTES). The design of the SC surfactant and the amine-terminated interlayer facilitates the assembly of SWCNTs and achieves over 90% effective coverage (**Figure 3c**). On the other hand, the ability of alkyl-chain-based surfactants to disperse SWCNTs in an ink yielded

poor assembly on the PLL-modified surface (**Figure 3d**). As a result, the combination of the SC surfactant and amine-terminated interlayer method is effective to assemble SWCNTs quickly, and a roll-to-roll printing of the active layer of the SWCNT network on PET substrate was demonstrated at a scale over 1 m in length (**Figure 3e**).

### **3. Flexible electronics for physical sensing**

The active printed or transferred materials discussed above have been widely used in the e-skin platform for physical sensing. Applications include strain & temperature sensors<sup>25,27,28</sup> electronic whiskers (e-whiskers),<sup>11,29</sup> and wearable devices<sup>30</sup>.

For the active matrix backplane of e-skin, nanomaterial-based transistor arrays using aligned nanowire arrays<sup>27</sup> or SWCNT network films<sup>12</sup> have been patterned for the switching function to select each pixel for tactile pressure readings. **Figure 4a** displays an e-skin based on aligned Ge/Si core/shell nanowire array transistors where the nanowire arrays are used as the transistor channel. <sup>27</sup> The transistors show a relatively high field-effect mobility of  $\sim 20$  cm<sup>2</sup>/Vs with an ON/OFF current ratio of about 100. Importantly, the transistors are mechanically stable even under a 2.5 mm bending radius and >2,000 bending cycles. Integrating a nanowire transistor array (18×19 pixels) for the active matrix and a conductive pressure sensitive rubber (PSR) (**Figure 4c**) enables tactile pressure mapping similar to that of human skin (**Figure 4d**). Although the conductive type PSR is used



for this application, other types of PSR using the mechanism of capacitance change or piezoelectric detection can be also applied to the e-skin.<sup>31</sup>

In addition to sensing, user-interactive functionalities are highly attractive for future electronic skin. Tactile pressure sensitive e-skin and organic light emitting diodes (OLEDs) can be integrated for instantaneous pressure visualization (**Figure 4e**).<sup>28</sup> An active matrix circuit consisting of an SWCNT network thin film transistor with a field-effect mobility of  $\sim 20 \text{ cm}^2/\text{Vs}$  was used to read the tactile pressure on each pixel (**Figure 4g-4h**). The emitted peak wavelength of OLED can be adjusted by changing the organic emissive materials. The device configuration was  $16 \times 16$  pixels, where each pixel has an SWCNT transistor, a PSR, and an OLED. As shown in **Figure 4j-4k**, OLEDs emit light when sufficient tactile pressure is applied over the pixel due to the conductivity change of PSR and the corresponding current change through the OLED.

The e-skin devices explained above are typically fabricated by standard photolithography and vacuum-based deposition techniques. For practical applications, macroscale flexible electronics, including e-skin, should be economically prepared on a large scale. In this regard, printing techniques (such as screen printing and gravure printing) hold great promise for future flexible electronics. The fully printed  $20 \times 20$  array CNT-based active matrix backplane integrated with a tactile pressure sensor on a PET film was demonstrated *via* a roll-to-plate gravure printing method.<sup>25</sup> The transistor

performances are  $4 \pm 2 \mu\text{A}/\text{mm}$ ,  $4 \pm 0.4$ , and  $0.8 \pm 0.3 \text{ cm}^2/\text{Vs}$  for the on-current normalized by width,  $\text{Log}(I_{\text{ON}}/I_{\text{OFF}})$ , and field-effect mobility, respectively. Such a printing technology is critical to demonstrate macroscale electronic skin toward flexible and wearable sensing.

**Figure 5a-5c** shows printed strain sensors - electronic whiskers (e-whiskers) using a mixture of a CNT paste and Ag nanoparticle (NP) ink on a PDMS film.<sup>11</sup> The strain sensing mechanism monitors the tunnel current between AgNPs, as described in **Figure 5c**.<sup>29</sup> When the film is deformed, the distance of AgNPs increases due to the tensile strain on the top surface of the PDMS film, resulting in a lower tunnel current. The electrical resistance of the strain sensor film increases (decreases) when the resistive change sensitivity is  $\sim 8\%/\text{Pa}$  under tensile (compressive) strain caused by nitrogen ( $\text{N}_2$ ) gas flow (**Figure 5d**). Next, seven e-whiskers were attached on a semi-sphere PDMS object with printed Ag interconnect electrodes (**Figure 5e**). By flowing  $\text{N}_2$  gas from one side, the gas flow distribution can be successfully monitored by the e-whisker array (**Figure 5f**). It should be noted that there are different approaches to demonstrate high sensitive strain or tactile sensors using carbon nanomaterials (CNT, graphene etc.) arranged by the device structures such as network or foam shapes.<sup>4,32,33</sup>

Such printed sensors can be applied as wearable healthcare patches. In **Figure 5g**, printed flexible strain sensors (functioning as a three-axis accelerator) were screen-printed on a PET film along with an

electrocardiogram (ECG), skin temperature, and ultraviolet (UV) sensors.<sup>30</sup> Here the ECG sensor was made of screen-printed Ag electrodes. The temperature sensor consisted of a mixture of CNTs and poly(3,4-ethylenedioxythiophene)polystyrene sulfonate (PEDOT:PSS). The UV sensor was made of a ZnO nanorod network thin film. Attaching the wearable device onto skin allows the UV light intensity, skin temperature, ECG signals, and human activities to be monitored simultaneously (**Figure 5h**).

As another type of pressure and strain sensors, liquid metal-based devices have been developed.<sup>17,20</sup> As shown in **Figures 6a**, a soft tactile diaphragm pressure sensor was developed based on microfluidic channels filled with Galinstan.<sup>17</sup> The diaphragm pressure sensor design utilizes a Wheatstone bridge circuit to measure small values of resistance changes caused by the applied pressure. The device had an ultra-low detection limit sub-100 Pa and was able to sense sub-50 Pa changes in pressure (**Figures 6b**). Furthermore, the Wheatstone bridge embedded in the diaphragm pressure sensor also provided temperature self-compensation in the operation range of 20-50 °C, which is critical for practical use considering that the temperature could have significant influences on the performance of resistive pressure sensors. The applications of such pressure sensor toward wearable sensing were demonstrated in the context of real-time heart rate monitoring *via* a PDMS wristband and tactile sensing *via* a PDMS glove.

In order to realize liquid-state devices and systems, different liquid components are required for controlled heterojunctions (**Figure 6c**),<sup>16</sup> analogous to metal-semiconductor or semiconductor-semiconductor junctions seen in conventional solid-state devices. In a liquid-liquid heterojunction, it is critical to prevent the breakdown of liquid heterointerfaces. Based on these considerations, a system for temperature and humidity sensing (**Figure 6d**) using Galinstan with highly robust liquid-state heterojunctions was developed.<sup>16</sup> The use of this liquid-state heterojunction and the ionic liquid as active sensing elements greatly expands the species of the liquid-state sensor.

Adding 2-dimensional (2D) fabrication methods such as soft lithography to a 3-dimensional (3D) printing method with liquid metals realizes good system-level fabrication methods toward physical sensing (**Figure 6e**).<sup>18</sup> One of the advantages of applying liquid metals as electrodes is easy fabrication of electrical interconnections in three dimensions with a stable contact between electrodes and electrical components in solid-state electronics such as ICs, resistors, and capacitors. In terms of liquid metal interconnections, only injections of liquid metals are required as long as the circuit designs of the microchannels for electrodes are optimized. A monolithic printed smart glove with a resistive heater and a wearable core body temperature was demonstrated (**Figure 6f**) based on 3D embedded liquid metal microchannels.<sup>19</sup>

#### 4. Flexible electronics for wearable chemical sensing

As most of the skin-interfaced flexible sensors reported so far primarily focused on monitoring of the user's physical activities and vital signs, there is a strong need of developing flexible devices that can capture molecular data from the human body to retrieve more insightful health information. In traditional clinical or laboratory settings, health examinations rely heavily on blood analysis, which is limited by invasive blood draws that cannot provide dynamic and continuous information. Human sweat is an important and easily accessible body fluid containing a wealth of chemicals that can reflect an individual's physiological state.<sup>34-42</sup> It has been shown that abnormal health conditions can significantly affect sweat composition by varying concentration of sweat analytes.<sup>37,39-41</sup> The transition from blood analysis to *in situ* sweat analysis *via* a wearable sweat sensor could provide a noninvasive and attractive means of dynamic health assessment.<sup>34-42</sup>

A number of wearable and flexible sweat sensors have recently been developed toward continuous health monitoring. Given the complex sweat secretion process, multiplexed and real-time detection of target biomarkers of interest is in urgent need. We proposed an integrated wearable and flexible sensor array for *in situ* sweat sensing.<sup>37</sup> This skin patch consists of multiple high-performance electrochemical sensors and a flexible printed circuit board (FPCB) for signal processing and wireless transmission. This device simultaneously measures sweat metabolites (lactate and glucose), sweat electrolytes ( $\text{Na}^+$  and  $\text{K}^+$ ), as well as skin temperature (**Figure 7**).<sup>37</sup>

The wearable system was able to monitor changes in physiologically relevant analytes over periods of prolonged exercise. The scope of this platform was later expanded to monitor a wide panel of analytes including pH, Ca<sup>2+</sup>, Cl<sup>-</sup>, heavy metals, and other substances.<sup>41-46</sup>

While sweat is easily accessible during vigorous physical exercise, its composition varies as the body undergoes fast physiological and metabolic changes. To this end, for medical applications, a promising sweat induction method is iontophoresis, which could be used to induce sweat excretion locally *via* chemical stimulation of the sweat gland. During iontophoresis, a small electric current will be applied to pass the charged substance (e.g., pilocarpine, acetylcholine, or methacholine) through intact skin which stimulates the secretion of sweat. A flexible sweat extraction and analysis platform has recently been demonstrated which contains a chemically enhanced iontophoresis module capable of autonomously inducing sweat (**Figure 8a**).<sup>41</sup> Through programming the drug concentrations in iontophoresis hydrogels and iontophoresis period, various sweat secretion profiles can be achieved. The integrated chemical sensors between iontophoresis electrodes can perform in situ analysis of the extracted sweat analytes.

It has been widely recognized that sweat compositions and sweat rate are inextricably linked.<sup>34,36,40</sup> In this regard, sweat rate monitoring will be crucial for both fundamental and clinical investigations. A flexible microfluidic sweat sensing patch has been developed recently for real-time sweat rate

monitoring and enhanced sweat analysis (**Figure 8b**).<sup>45</sup> The electrical impedance magnitude between two parallel electrodes in the microchannel drops as sweat fills the microchannel. Sweat rate could be calculated as sweat volume change in the channel divided by the time interval. The use of microfluidic systems can minimize the sweat evaporation and contamination, resulting in more accurate sweat sensing with higher temporal resolution.

In practical health monitoring applications, high-throughput and low-cost fabrication of flexible sensors with high stability and reproducibility is critical for the commercial adoption of future wearable sensors.<sup>47,48</sup> In this regard, roll-to-roll (R2R) gravure printing technology has been exploited to print high-performance flexible sensing electrodes on 150 m flexible substrate rolls (**Figure 8c**).<sup>47</sup> These electrodes can be used to prepare flexible sensors for analyzing sweat metabolites, ions, and other substances. Such R2R gravure printing technology represents a significant step in enabling low-cost mass production of future wearable and flexible sensors.

The development of wearable sweat sensors opens the door to physiological and biomedical monitoring applications. We recently showed that such wearable sensor could potentially be used for real-time monitoring of dehydration during prolonged physical exercise (**Figure 9a**).<sup>37</sup> Sweat Na<sup>+</sup> levels remained stable during euhydration trials while substantial increases in sweat Na<sup>+</sup> levels were observed when the subjects had lost a large amount of water during the outdoor running. The use of the sweat sensor for cystic fibrosis screening and early diagnosis was successfully demonstrated

by detecting elevated sweat electrolyte ( $\text{Na}^+$  and  $\text{Cl}^-$ ) levels (**Figure 9b**).<sup>41</sup> Wearable sweat sensors are shown to have great promise in dynamic drug monitoring for precision medicine. Elevated caffeine levels in sweat upon increasing drug dosage and confirmable caffeine physiological trends were observed (**Figure 9c**).<sup>46</sup> The wearable devices allow investigating the dynamic correlation between sweat and blood analyte levels. Our preliminary data showed that oral glucose consumption resulted in an increase of sweat glucose level for most of the fasting subjects (**Figure 9d**).<sup>41</sup>

## **5. Conclusion and outlook**

In this Account, we have reviewed and highlighted the latest scientific and technical advances in flexible electronic devices toward wearable physical and chemical sensing. Such skin-interfaced flexible sensors have promising prospects in personalized healthcare as they provide affordable and non-invasive solutions for health monitoring, early diagnosis, and disease management beyond traditional controlled laboratory settings. Despite the significant progress, a major hurdle in this field is the lack of robust wearable sensing systems that can accurately and continuously collect data from the human body. Novel materials, sensing techniques, and seamless system integration strategies need to be explored for realizing the full potential of flexible electronics toward wearable sensing. Future work should also focus on human studies to determine how the measured physical and chemical information relate to the individual's health status. Considering the complexity of the human body, skin-interfaced flexible systems that can



monitor both biomolecular levels and vital signs (e.g., blood pressure, heart rate, respiratory rate, and body temperature) represent an attractive solution for accurately predicting and identifying more specific health conditions. Further research in these directions, along with the large sets of data collected from the population studies *via* these wearable sensing technologies, will have a significant impact on personalized healthcare.

### **Biographical Information**

Wei Gao received his Ph.D. degree in Chemical Engineering from University of California in 2014, San Diego, and performed his postdoctoral work at University of California, Berkeley between 2014 and 2017. He is currently an assistant professor of medical engineering at California Institute of Technology. His research focuses on biosensors, flexible electronics and micro/nanomachines.

Hiroki Ota received his Ph.D. degree in Mechanics at Keio University, Japan in 2011, and performed his postdoctoral work at Tokyo Women's Medical University-Waseda University Joint Institution for Advanced Biomedical Sciences and University of California, Berkeley. He is currently an associate professor in Yokohama National University. His current research focuses on flexible sensors/actuators using liquid metal and smart device for healthcare.

Daisuke Kiriya received his PhD degree in Engineering from Kyoto University, Japan in 2009, and performed his postdoctoral work at the University of Tokyo from 2009 to 2012 and the University of California, Berkeley between

2012 and 2016. He is currently an assistant professor in the department of physics and electronics at Osaka Prefecture University, Japan. His research focuses on molecular modification of nanomaterials and 2D material devices.

Kuniharu Takei received his Ph.D. degree in 2009 from Toyohashi University of Technology, Japan and performed his postdoctoral work at University of California, Berkeley between 2009 and 2013. He is currently an associate professor of the department of physics and electronics at Osaka Prefecture University, Japan. His research focuses on flexible printed electronics and device physics.

Ali Javey received his Ph.D. degree in chemistry from Stanford University in 2005 and was a Junior Fellow of the Harvard Society of Fellows from 2005 to 2006. He then joined the faculty of the University of California at Berkeley where he is currently a professor of Electrical Engineering and Computer Sciences. He is also a faculty scientist at the Lawrence Berkeley National Laboratory where he serves as the program leader of Electronic Materials (E-Mat). He is an associate editor of ACS Nano.

## **REFERENCES**

1. Rogers, J. A.; Someya, T.; Huang, Y. Materials and mechanics for stretchable electronics. *Science* 2010, 327, 1603-1607.
2. Someya, T.; Bao, Z.; Malliaras, G. G. The Rise of Plastic Bioelectronics. *Nature* 2016, 540, 379- 385.

3. Kim, D.-H.; Lu, N.; Ma, R.; Kim, Y.-S.; Kim, R.-H.; Wang, S.; Wu, J.; Won, S. M.; Tao, H.; Islam, A.; Yu, K. J.; Kim, T.-i.; Chowdhury, R.; Ying, M.; Xu, L.; Li, M.; Chung, H.-J.; Keum, H.; McCormick, M.; Liu, P.; Zhang, Y.-W.; Omenetto, F. G.; Huang, Y.; Coleman, T.; Rogers, J. A. Epidermal Electronics. *Science* 2011, 333, 838-843.
4. Lipomi, D. J.; Vosgueritchian, M.; Tee, B. C.; Hellstrom, S. L.; Lee, J. A.; Fox, C. H.; Bao, Z. Skin-Like Pressure and Strain Sensors Based on Transparent Elastic Films of Carbon Nanotubes. *Nat. Nanotechnol.* 2011, 6, 788-792.
5. Lüssem, B.; Keum, C.-M.; Kasemann, D.; Naab, B.; Bao, Z.; Leo, K. Doped Organic Transistors. *Chem. Rev.* **2016**, 116, 13714-13751.
6. Chen, K.; Gao, W.; Emaminejad, S.; Kiriya, D.; Ota, H.; Nyein, H. Y. Y.; Takei, K.; Javey, A. Printed Carbon Nanotube Electronics and Sensor Systems. *Adv. Mater.* **2016**, 28, 4397- 4414.
7. Kim, K. S.; Zhao, Y.; Jang, H.; Lee, S. Y.; Kim, J. M.; Kim, K. S.; Ahn, J. H.; Kim, P.; Choi, J. Y.; Hong, B. H. Large-Scale Pattern Growth of Graphene Films for Stretchable Transparent Electrodes *Nature* **2009**, 457, 706-710.
8. Takahashi, T.; Takei, K.; Adabi, E.; Fan, Z.; Niknejad, A. M.; Javey, A. Parallel Array InAs Nanowire Transistors for Mechanically Bbendable, Ultrahigh Frequency Electronics. *ACS Nano* **2010**, 4, 5855-5860.
9. Fan, Z.; Ho, J. C.; Takahashi, T.; Yerushalmi, R.; Takei, K.; Ford, A. C.; Chueh, Y.-L.; Javey, A. Toward the Development of Printable Nanowire Electronics and Sensors. *Adv. Mater.* **2009**, 21, 3730-3743.

10. Nomura, K.; Nomura, K.; Ohta, H.; Takagi, A.; Kamiya, T.; Hirano, M.; Hosono, H. Room-Temperature Fabrication of Transparent Flexible Thin-Film Transistors using Amorphous Oxide Semiconductors. *Nature* **2004**, *432*, 488-492.
11. Takei, K.; Takahashi, T.; Ho, J. C.; Ko, H.; Gillies, A. G.; Leu, P. W.; Fearing, R. S.; Javey, A. Highly Sensitive Electronic Whiskers based on Patterned Carbon Nanotube and Silver Nanoparticle Composite Films. *Proc. Natl. Acad. Sci. U. S. A.* **2014**, *111*, 1703-1707.
12. Takahashi, T.; Takei, K.; Gillies, A. G.; Fearing, R. S.; Javey, A. Carbon Nanotube Active-Matrix Backplanes for Conformal Electronics and Sensors. *Nano Lett.* **2011**, *11*, 5408-5413.
13. Sangwan, V. K.; Ortiz, R. P.; Alaboson, J. M. P.; Emery, J. D.; Bedzyk, M. J.; Lauhon, L. J.; Marks, T. J.; Hersam, M. C. Fundamental Performance Limits of Carbon Nanotube Thin-Film Transistors Achieved Using Hybrid Molecular Dielectrics. *ACS Nano* **2012**, *6*, 7480-7488.
14. Kiriya, D.; Chen, K.; Ota, H.; Lin, Y. J.; Zhao, P. D.; Yu, Z. B.; Ha, T. J.; Javey, A. Design of Surfactant-Substrate Interactions for Roll-to-Roll Assembly of Carbon Nanotubes for Thin-Film Transistors. *J. Am. Chem. Soc.* **2014**, *136*, 11188-11194.
15. Daeneke, T.; Khoshmanesh, K.; Mahmood, N.; de Castro, I. A.; Esrafilzadeh, D.; Barrow, S. J.; Dickey, M. D.; Kalantar-zadeh, K. Liquid Metals: Fundamentals and Applications in Chemistry. *Chem. Soc. Rev.* **2018**, *47*, 4073-4111.

16. Ota, H.; Chen, K.; Lin, Y.; Kiriya, D.; Shiraki, H.; Yu, Z.; Ha, T.-J.; Javey, A. Highly Deformable Liquid-State Heterojunction Sensors. *Nat. Commun.* **2014**, *5*, 5032.
17. Gao, Y.; Ota, H.; Schaler, E. W.; Chen, K.; Zhao, A.; Gao, W.; Fahad, H. M.; Leng, Y.; Zheng, A.; Xiong, F.; Zhang, C.; Tai, L.-C.; Zhao, P.; Fearing, R. S.; Javey, A. Wearable Microfluidic Diaphragm Pressure Sensor for Health and Tactile Touch Monitoring. *Adv. Mater.* **2017**, *29*, 1701985.
18. Ota, H.; Emaminejad, S.; Gao, Y.; Zhao, A.; Wu, E.; Challa, S.; Chen, K.; Fahad, H. M.; Jha, A. K.; Kiriya, D.; Gao, W.; Shiraki, H.; Morioka, K.; Ferguson, A. R.; Kealy, K. E.; Davis, R. W.; Javey, A. 3D Printing: Application of 3D Printing for Smart Objects with Embedded Electronic Sensors and Systems. *Adv. Mater. Technol.* **2016**, *1*, 1600013.
19. Ota, H.; Chao, M.; Gao, Y.; Wu, E.; Tai, L.-C.; Chen, K.; Matsuoka, Y.; Iwai, K.; Fahad, H. M.; Gao, W.; Nyein, H. Y. Y.; Lin, L.; Javey, A. 3D Printed “Earable” Smart Devices for Real-Time Detection of Core Body Temperature. *ACS Sens.* **2017**, *2*, 990-997.
20. Y. Park; B. Chen; R. J. Wood. Design and Fabrication of Soft Artificial Skin Using Embedded Microchannels and Liquid Conductors. *IEEE Sens. J.* **2012**, *12*, 2711-2718.
21. Yerushalmi, R.; Jacobson, Z. A.; Ho, J. C.; Fan, Z.; Javey, A. Large Scale, Highly Ordered Assembly of Nanowire Parallel Arrays by Differential Roll Printing. *Appl. Phys. Lett.* **2007**, *91*, 203104.

22. Fan, Z.; Ho, J. C.; Jacobson, Z. A.; Razavi, H.; Javey, A. Large-Scale, Heterogeneous Integration of Nanowire Arrays for Image Sensor Circuitry. *Proc. Natl. Acad. Sci. U. S. A.* **2008**, *105*, 11066-11070.
23. Arias, A. C.; MacKenzie, J. D.; McCulloch, I.; Rivnay, J.; Salleo, A. Materials and Applications for Large Area Electronics: Solution-Based Approaches. *Chem. Rev.* **2010**, *110*, 3-24.
24. Fujisaki, Y.; Koga, H.; Nakajima, Y.; Nakata, M.; Tsuji, H.; Yamamoto, T.; Kurita, T.; Nogi, M.; Shimidzu, N. Transparent Nanopaper-Based Flexible Organic Thin-Film Transistor Array. *Adv. Funct. Mater.* **2014**, *24*, 1657-1663.
25. Yeom, C.; Chen, K.; Kiriya, D.; Yu, Z.; Cho, G.; Javey, A. Large-Area Compliant Tactile Sensors Using Printed Carbon Nanotube Active-Matrix Backplanes. *Adv. Mater.* **2015**, *27*, 1561-1566.
26. Sangwan, V.; Behnam, A.; Ballarotto, V.; Fuhrer, M.; Ural, A.; Williams, E. Optimizing Transistor Performance of Percolating Carbon Nanotube Networks. *Appl. Phys. Lett.* **2010**, *97*, 043111.
27. Takei, K.; Takahashi, T.; Ho, J. C.; Ko, H.; Gillies, A. G.; Leu, P. W.; Fearing, R. S.; Javey, A. Nanowire Active-Matrix Circuitry for Low-Voltage Macroscale Artificial Skin. *Nat. Mater.* **2010**, *9*, 821- 826.
28. Wang, C.; Hwang, D.; Yu, Z.; Takei, K.; Park, J.; Chen, T.; Ma, B.; Javey, A. User Interactive Electronic Skin for Instantaneous Pressure Visualization. *Nat. Mater.* **2013**, *12*, 899-904.

29. Harada, S.; Honda, W.; Arie, T.; Akita, S.; & Takei, K. Fully Printed, Highly Sensitive Multifunctional Artificial Electronic Whisker Arrays Integrated with Strain and Temperature Sensors. *ACS Nano* **2014**, *8*, 3921-3927.
30. Yamamoto, Y.; Harada, S.; Yamamoto, D.; Honda, W.; Arie, T.; Akita, S.; Takei, K. Printed Multifunctional Flexible Device with an Integrated Motion Sensor for Health Care Monitoring. *Sci. Adv.* **2016**, *2*, e1601473.
31. Chortos, A.; Liu, J.; Bao, Z. Pursuing Prosthetic Electronic Skin. *Nat. Mater.* **2016**, *15*, 937-950.
32. Chen, Z.; Ren, W.; Gao, L.; Liu, B.; Pei, S.; Cheng, H. M. Three-Dimensional Flexible and Conductive Interconnected Graphene Networks Grown by Chemical Vapour Deposition. *Nature Mater.* **2011**, *10*, 424-428.
33. Li, W.; Guo, J.; Fan, D, 3D Graphite-Polymer Flexible Strain Sensors with Ultrasensitivity and Durability for Real-Time Human Vital Sign Monitoring and Musical Instrument Education. *Adv. Mater. Tech.* **2017**, *2*, 1700070.
34. Bariya, M.; Nyein, H. Y. Y.; Javey, A. Wearable Sweat Sensors. *Nat. Electron.* **2018**, *1*, 160-171.
35. Bandodkar, A. J.; Jeerapan, J.; Wang, J. Wearable Chemical Sensors: Present Challenges and Future Prospects, *ACS Sens.* **2016**, *1*, 464-482.
36. Yang, Y.; Gao, W. Wearable and Flexible Electronics for Continuous Molecular Monitoring. *Chem. Soc. Rev.* **2018**, 10.1039/c7cs00730b.

37. Gao, W.; Emaminejad, S.; Nyein, H. Y. Y.; Challa, S.; Chen, K.; Peck, A.; Fahad, H. M.; Ota, H.; Shiraki, H.; Kiriya, D.; Lien, D.-H.; Brooks, G. A.; Davis, R. W.; Javey, A. Fully Integrated Wearable Sensor Arrays for Multiplexed In Situ Perspiration Analysis. *Nature* **2016**, *529*, 509-514.
38. Koh, A.; Kang, D.; Xue, Y.; Lee, S.; Pielak, R. M.; Kim, J.; Hwang, T.; Min, S.; Banks, A.; Bastien, P.; Manco, M. C.; Wang, L.; Ammann, K. R.; Jang, K.-I.; Won, P.; Han, S.; Ghaffari, R.; Paik, U.; Slepian, M. J.; Balooch, G.; Huang, Y.; Rogers, J. A. A Soft, Wearable Microfluidic Device for the Capture, Storage, and Colorimetric Sensing of Sweat. *Sci. Transl. Med.* **2016**, *8*, 366ra165.
39. Lee, H.; Choi, T. K.; Lee, Y. B.; Cho, H. R.; Ghaffari, R.; Wang, L.; Choi, H. J.; Chung, T. D.; Lu, N.; Hyeon, T.; Choi, S. H.; Kim, D. H. A Graphene-Based Electrochemical Device with Thermoresponsive Microneedles for Diabetes Monitoring and Therapy. *Nat. Nanotechnol.* **2016**, *11*, 566-572.
40. Heikenfeld, J. Non-invasive Analyte Access and Sensing through Eccrine Sweat: Challenges and Outlook circa 2016. *Electroanalysis* **2016**, *28*, 1242-1249.
41. Emaminejad, S.; Gao, W.; Wu, E.; Davies, Z. A.; Yin Yin Nyein, H.; Challa, S.; Ryan, S. P.; Fahad, H. M.; Chen, K.; Shahpar, Z.; Talebi, S.; Milla, C.; Javey, A.; Davis, R. W. Autonomous Sweat Extraction and Analysis Applied to Cystic Fibrosis and Glucose Monitoring Using a Fully Integrated Wearable Platform. *Proc. Natl. Acad. Sci. U. S. A.* **2017**, *114*, 4625-4630.



42. Gao, W.; Nyein, H. Y. Y.; Shahpar, Z.; Fahad, H. M.; Chen, K.; Emaminejad, S.; Gao, Y.; Tai, L.-C.; Ota, H.; Wu, E.; Bullock, J.; Zeng, Y.; Lien, D.-H.; Javey, A. Wearable Microsensor Array for Multiplexed Heavy Metal Monitoring of Body Fluids. *ACS Sens.* **2016**, *1*, 866-874.
43. Nyein, H. Y. Y.; Gao, W.; Shahpar, Z.; Emaminejad, S.; Challa, S.; Chen, K.; Fahad, H. M.; Tai, L.-C.; Ota, H.; Davis, R. W.; Javey, A. A Wearable Electrochemical Platform for Noninvasive Simultaneous Monitoring of  $\text{Ca}^{2+}$  and pH. *ACS Nano* **2016**, *10*, 7216-7224.
44. Nakata, S.; Arie, T.; Akita, S.; Takei, K. Wearable, Flexible, and Multifunctional Healthcare Device with an ISFET Chemical Sensor for Simultaneous Sweat pH and Skin Temperature Monitoring. *ACS Sens.* **2017**, *2*, 443-448.
45. Nyein, H. Y. Y.; Tai, L.-C.; Ngo, Q. P.; Chao, M.; Zhang, G.; Gao, W.; Bariya, M.; Bullock, J.; Kim, H.; Fahad, H. M.; Javey, A. A Wearable Microfluidic Sweat Sensing Patch for Dynamic Sweat Secretion Analysis. *ACS Sens.* **2018**, *3*, 944-952.
46. Tai, L.-C., Gao, W., Chao, M., Bariya, M., Ngo, Q. P., Shahpar, Z., Nyein, H. Y. Y., Park, H., Sun, J., Jung, Y., Wu, E., Fahad, H. M., Lien, D.-H., Ota, H., Cho, G., Javey, A. Methylxanthine Drug Monitoring with Wearable Sweat Sensors. *Adv. Mater.* **2018**, *30*, 1707442.
47. Bariya, M.; Shahpar, Z.; Park, H.; Sun, J.; Jung, Y.; Gao, W.; Nyein, H. N.; Liaw, T. S.; Tai, L.-C.; Ngo, Q. P.; Chao, M.; Zhao, Y.; Hettick, M.; Cho, G.;

Javey, A. Roll-to-Roll Gravure Printed Electrochemical Sensors for Wearable and Medical Devices. *ACS Nano* **2018**, *12*, 6978-6987.

48. Nassar, J. M.; Cordero, M. D.; Kutbee, A. T.; Karimi, M. A.; Torres Sevilla, G. A.; Hussain, A. M.; Shamim, A.; Hussain, M. M. Paper Skin Multisensory Platform for Simultaneous Environmental Monitoring. *Adv. Mater. Tech.* **2016**, *1*, 1600004.

# FIGURES

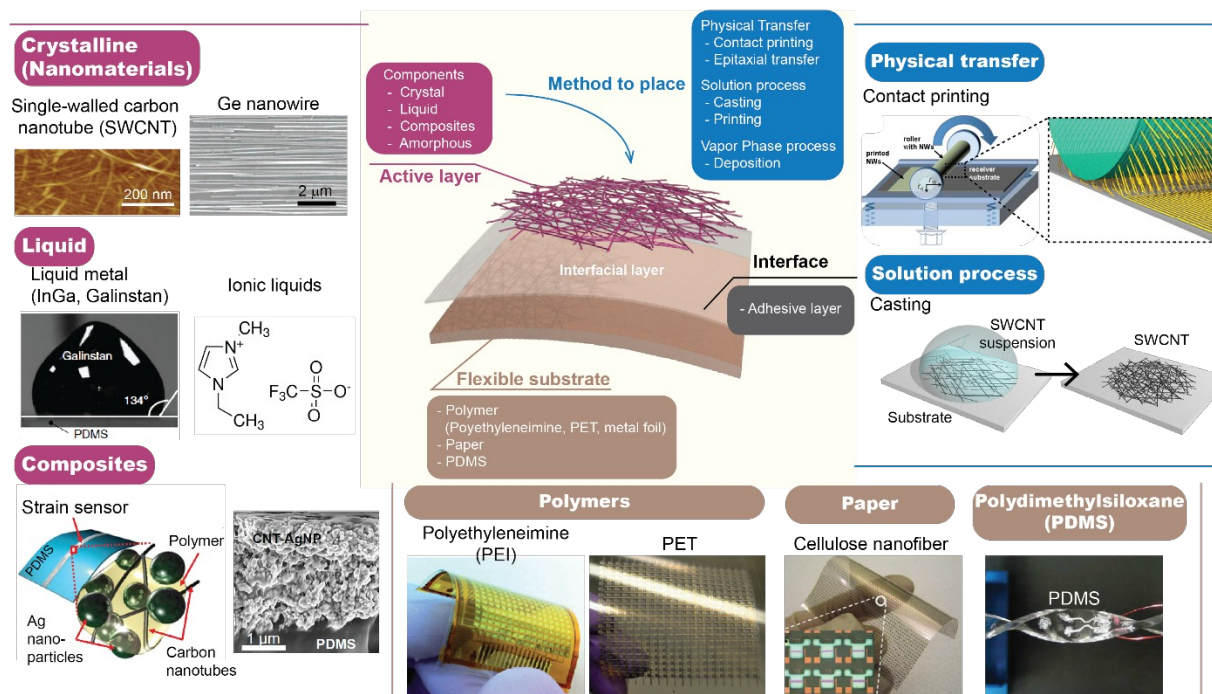


**Figure 1.** Materials of electronic skin toward wearable physical and chemical sensing. The devices are constructed by the substrates, the active layers to

functionalize and the adhesive layer to keep the active layer. The transfer method should be considered to construct the active layer. Reproduced with permission from ref. 9. Copyright 2009 Wiley. Reproduced with permission from ref. 11. Copyright 2014 National Academy of Sciences. Reproduced with permission from ref. 14. Copyright 2014 American Chemical Society. Reproduced with permission from ref. 16. Copyright 2014 Nature Publishing Group. Reproduced with permission from ref. 24. Copyright 2014 Wiley. Reproduced with permission from ref. 25. Copyright 2015 Wiley. Reproduced with permission from ref. 28. Copyright 2013 Nature Publishing Group.

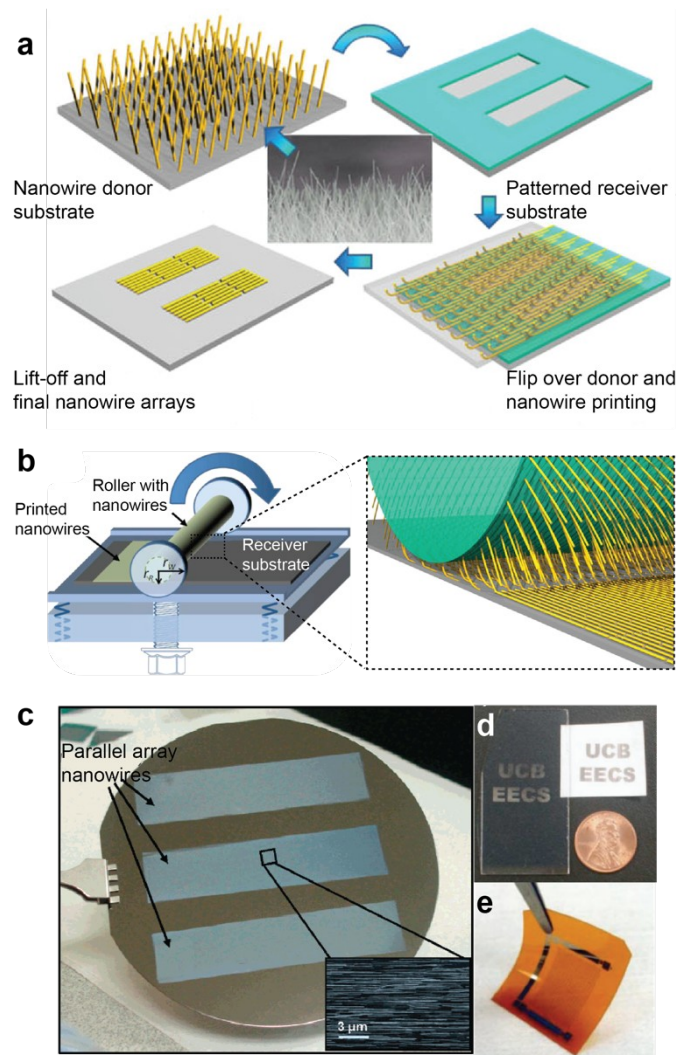


**Figure 2.** Physical transfer processes of nanowires. (a) Ge nanowires were transferred *via* contact shearing. (b) Illustrative image of the roll-contact printing. (c-e) Images of the nanowire-transferred (c) wafer, (d) glass and paper, and (e) flexible PEI substrates. Reproduced with permission from ref. 9. Copyright 2009 Wiley.

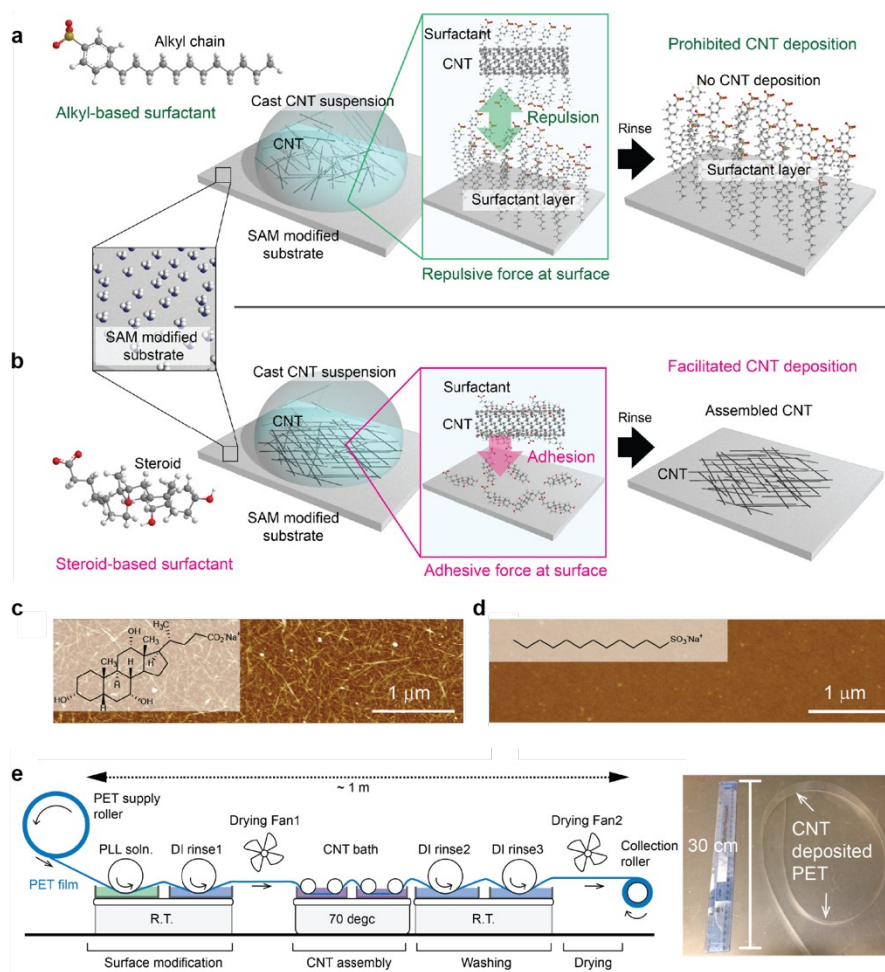


**Figure 3.** Solution process to transfer SWCNTs. (a) Alkyl-chain-type interlayer (surfactant) shows no deposition and (b) cholate-type interlayer (surfactant) shows effective assembly of SWCNTs. (c-d) Atomic force microscope images of the interlayer (surfactant) of (c) sodium cholate and (d) sodium dodecyl sulfate. (e) Roll-to-roll printing of the SWCNTs. Reproduced with permission from ref. 14. Copyright 2014 American Chemical Society.

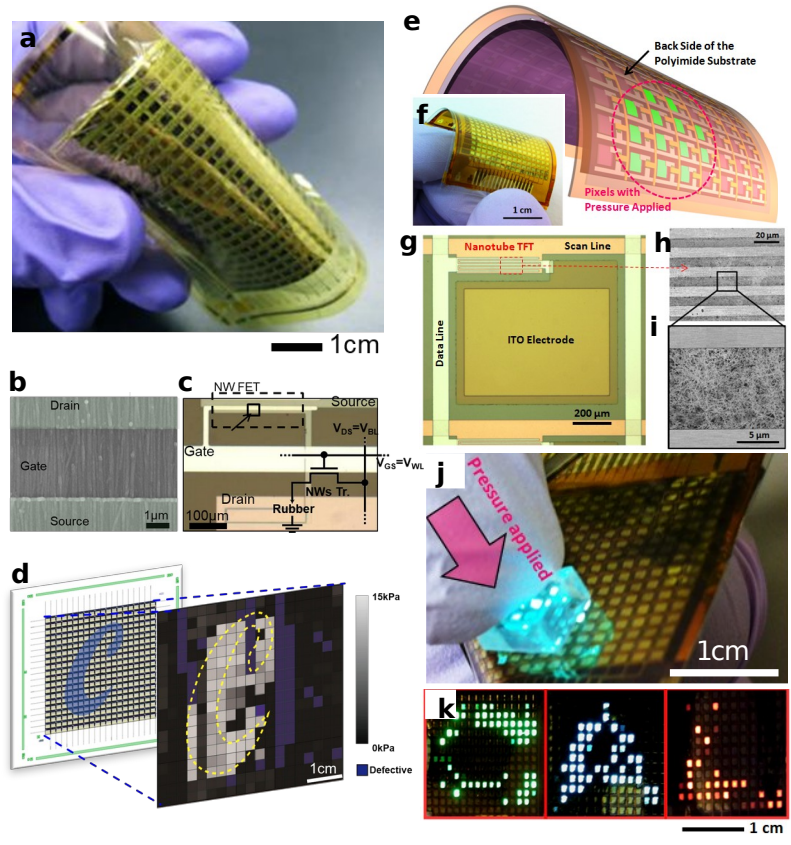


**Figure 4.** Interactive electronic skin. (a) Photo of the Ge/Si core/shell nanowire array-based active matrix e-skin. (b) SEM image of the aligned nanowire array in the transistor channel and (c) photo of the pixel. Inset shows the circuit diagram of the pixel. (d) Tactile pressure mapping results. Reproduced with permission from ref. 27. Copyright 2010 Nature Publishing Group. (e) Schematic and (f) photo of the tactile responsive e-skin. (g) Photo of a pixel and (h) (i) enlarged SEM images of the SWCNT network transistor channels. (j) Light-emissive responsive e-skin demonstration. (k) Green, blue, and red light emissive displays due to applying tactile pressure. Reproduced with permission from ref. 28. Copyright 2013 Nature Publishing Group.

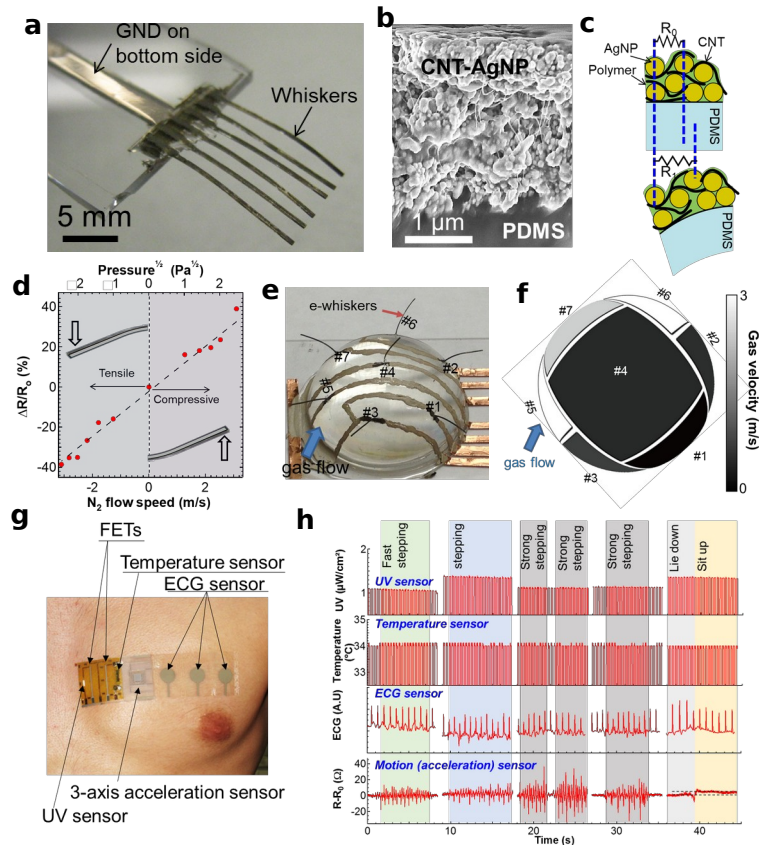


**Figure 5.** Flexible electronic devices for pressure sensing. (a) Fully printed artificial electronic whiskers. (b) SEM images of the CNTs and the AgNP composite film of the strain sensor. (c) Strain sensing mechanism. (d) Normalized resistance change ratio as functions of  $N_2$  gas flow rate and pressure. (e) e-whisker array demonstration and (f) gas flow distribution mapping result. Reproduced with permission from ref. 11. Copyright 2014 National Academy of Sciences. (g) Flexible healthcare patch sheet and (h) real-time multiple sensing results of UV, skin temperature, ECG, and human motion. Reproduced with permission from ref. 30. 2016 American Association for the Advancement of Science.



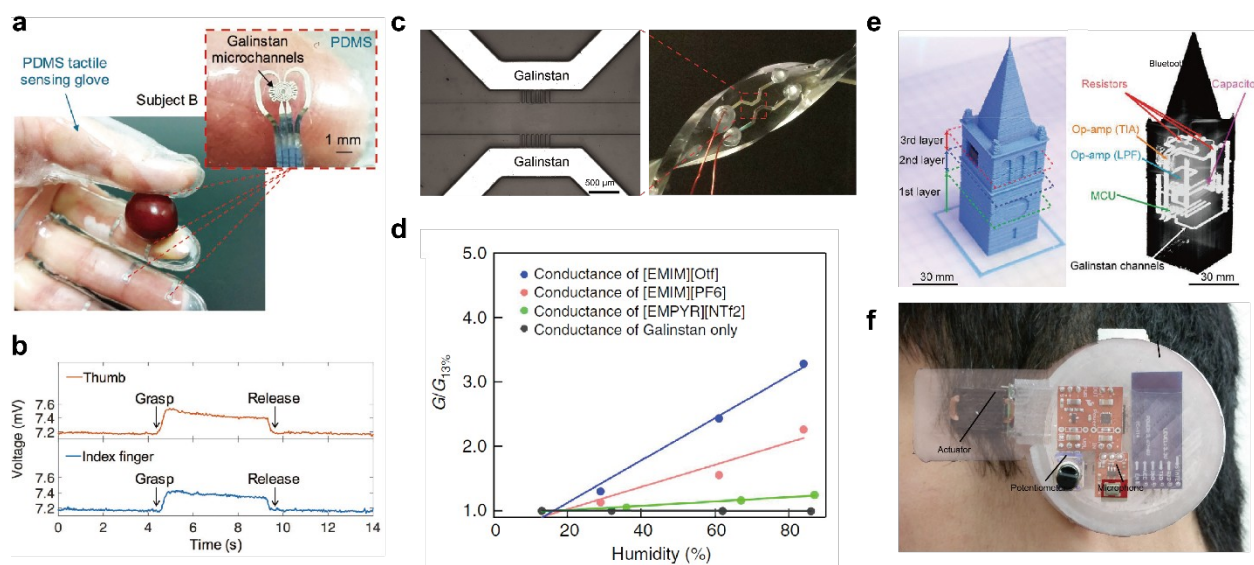


**Figure 6.** Liquid-based flexible electronics for wearable sensing. (a) A Microfluidic tactile diaphragm pressure sensor. (b) Real-time pressure sensing response recorded during gentle grasp and release. Reproduced with permission from ref. 17. Copyright 2017 Wiley. (c) Liquid-state heterojunction sensor. (d) Humidity sensor using liquid-state heterojunctions.

Reproduced with permission from ref. 16. Copyright 2014 Nature Publishing Group. (e) Optical and X-ray images of a 3D printed photodetection system. Reproduced with permission from ref. 18. Copyright 2016 Wiley. (f) A 3D printed earable device for core body temperature detection with Galinstan electrodes and interconnects. Reproduced with permission from ref. 19. Copyright 2017 American Chemical Society.

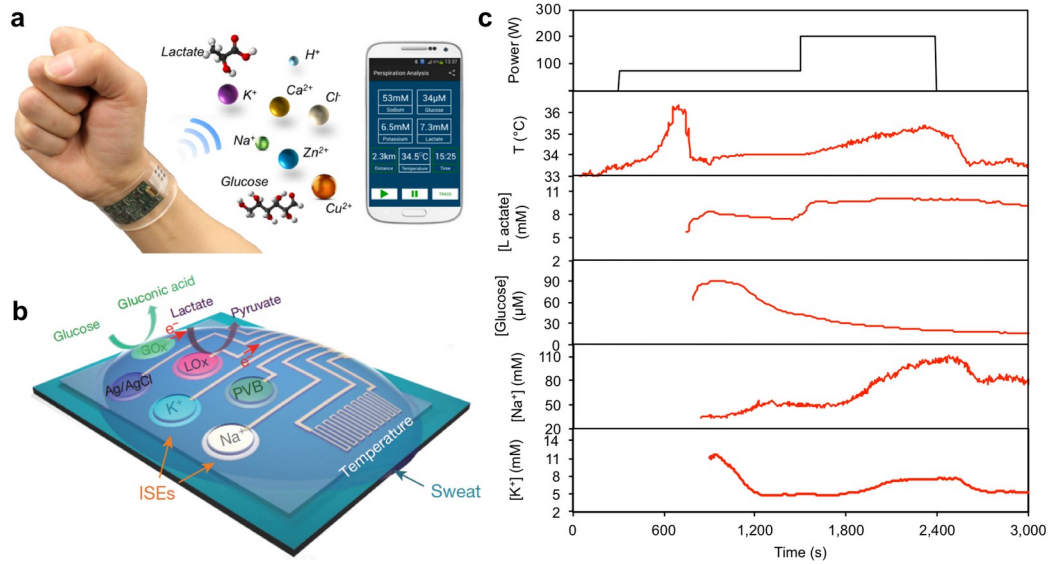


**Figure 7.** Wearable sweat sensor. (a) A fully-integrated flexible sweat sensor array. (b) Schematic of a sensor array for monitoring of sweat metabolites and electrolytes. (c) Real-time sweat analysis using during a cycling exercise. Reproduced with permission from ref. 37. Copyright 2016 Nature Publishing Group.

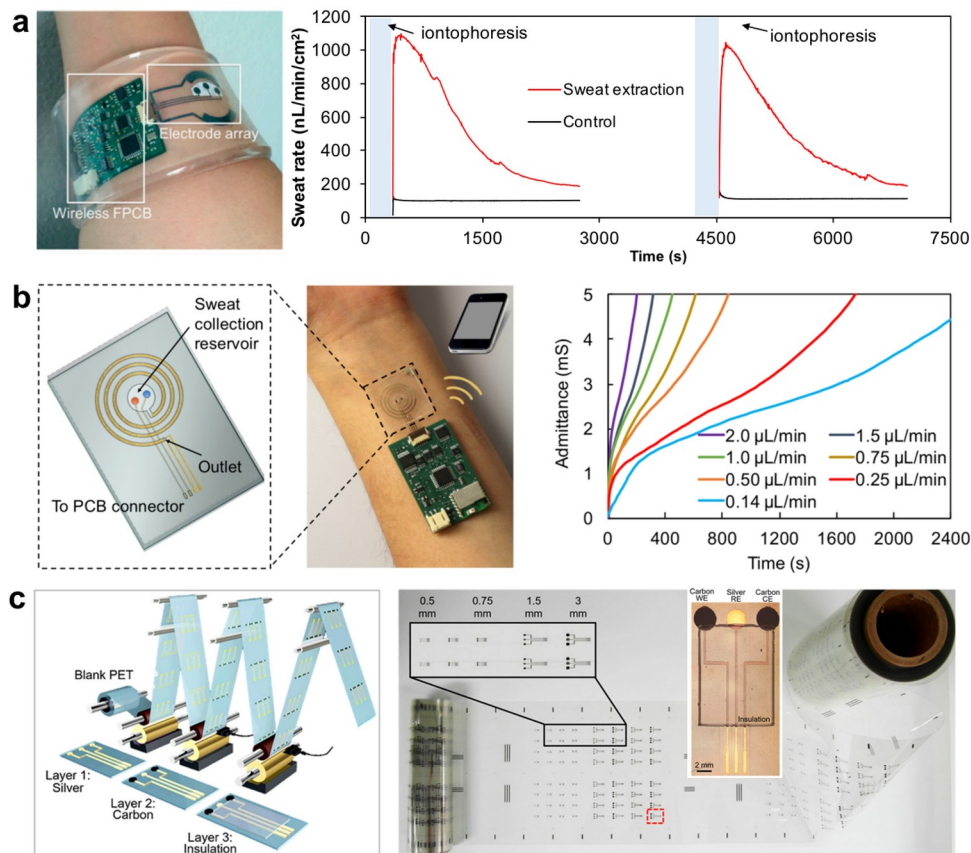


**Figure 8.** Effort toward enhancing sweat induction, sampling and sensing. (a) Wearable sensor with an integrated iontophoresis module toward autonomous sweat extraction. Reproduced with permission from ref. 41. Copyright 2017 National Academy of Sciences USA. (b) Microfluidic based sensing system for sweat sampling, sensing and sweat rate analysis. Reproduced with permission from ref. 45. Copyright 2018 American Chemical Society. (c) Roll-to-roll gravure printing enabled mass production of high-performance flexible chemical sensors at low cost. Reproduced with permission from ref. 47. Copyright 2018 American Chemical Society.

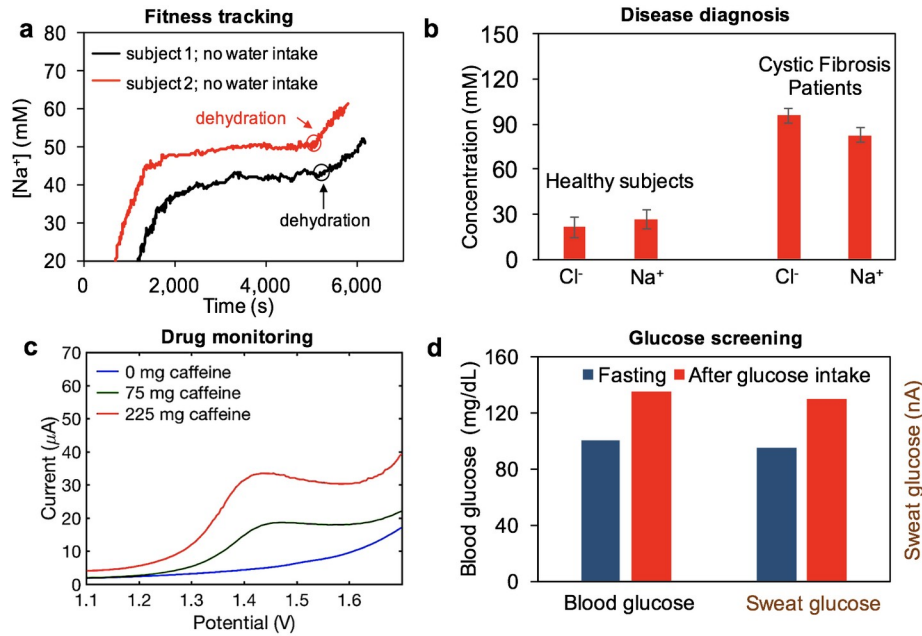


**Figure 9.** Physiological and biomedical applications of wearable & flexible sweat sensors. (a) Dehydration monitoring during physical exercise. Reproduced with permission from refs. 37. Copyright 2016 Nature Publishing Group. (b) Screening and diagnosis of cystic fibrosis. Reproduced with permission from ref. 41. Copyright 2017 National Academy of Sciences. (c) Dynamic drug (i.e., caffeine) monitoring. Reproduced with permission from ref. 46. Copyright 2018 Wiley. (d) A correlation study of sweat and blood glucose levels toward non-invasive glucose monitoring. Reproduced with permission from ref. 41. Copyright 2017 National Academy of Sciences.

# Conspectus graphic

